Experimental study of the Gaseous and Particulate Matter Emissions from a Gas Turbine Combustor burning butyl butyrate and ethanol blends

Longfei Chen [a], Zhichao Zhang [a,b,*], Yiji Lu [b,*], Chi Zhang [a], Xin Zhang [a], Cuiqi Zhang [a], Anthony Paul Roskilly [b]

[a] *School of Energy and Power Engineering, Energy and Environment International Center, Beihang University, Beijing, 100191, China*

[b] *Sir Joseph Swan Centre for Energy Research, Newcastle University, Newcastle, NE1 7RU, UK*

H I G H L I G H T S

- Study of using four butyl butyrate based biofuels for aviation application
- Two operational conditions (cruising and idling state) were studied
- Comprehensive emission and ion analysis were conducted

Abstract

This paper reports the gaseous pollutants and Particulate Matter (PM) emissions of a gas turbine combustor burning butyl butyrate and ethanol blends. The gas turbine has been tested under two operational conditions to represent the cruising (condition 1) and idling (condition 2) conditions of aero engines. Aviation kerosene RP-3 and four different biofuels using butyl butyrate (BB) and ethanol blends were tested and compared to evaluate the impact of fuel composition on CO, NO_x, unburnt hydrocarbon (UHC) and PM emissions under selected two operational conditions. The PM number (PN) concentration and size distributions were measured by a scanning mobility particle sizer (SMPS). The compositions of filter borne PM were analysed by ion chromatograph technique. The concentrations of CO, NO_x and UHC were detected and analysed by a gas analyser. Results indicated that under idling and cruising conditions the CO emissions from butyl butyrate and ethanol blends were higher than that of RP-3 due to the relatively lower combustion temperature of the biofuels compared with that of RP-3. Results of the NO_x emission comparison indicated the biofuels produced less NO_x than RP-3 and the increase of ethanol content in the biofuels could reduce the NO_x and UHC emissions. The particles smaller than 20 nm played a dominant role in PN emissions at condition 1 with the range from $2\times10^6/cm^3$ to $4\times10^7/cm^3$. There was a peak value of particle number concentration with the particle size ranging from about 25 nm and 40 nm. The PN emission index at condition 1 was higher than that at condition 2 for the biofuels, whilst the trend was opposite to that of RP-3. The ions analysis indicated Ca^{2+} and SO_4^{2-} were

* Corresponding author. Tel.: +44 (0) 191 208 4827
E-mail address: z.zhang34@ncl.ac.uk; zczhang1988@live.com (Z. Zhang)
yiji.lu@ncl.ac.uk; luyiji0620@gmail.com (Y. Lu)

the two dominant ions in the PM emissions of biofuels.

Keywords: gaseous emissions, particulate matter (PM), particle number (PN), butyl butyrate and ethanol blends, ions analysis

1. Introduction

The gaseous pollutants and particulate matters (PM) from burning fossil fuels have attracted ever increasing research attentions on the development of new fuel formulations [1-3], advanced engine design and calibration methods [4-6], and effective after treatment technologies [7, 8]. Increasingly strict emission regulations have been proposed and adopted including Euro V and VI requiring a non-volatile particle number (PN) emission limit of 6×10^{11} particles/km to complement the mass-based limit for PM emissions from light-duty diesel vehicles [9, 10]. Similar to vehicular emission regulations, the Committee on Aviation Environmental Protection (CAEP), a technical committee of the International Civil Aviation Organization (ICAO) Council has recently proposed amendments of number-based particle limits regarding the non-volatile Particulate Matter Standard [11]. The literature on aviation emission characteristics and their mitigation technologies is much scarcer compared with vehicular emissions. It is conceivable that the emissions from aviation gas turbine engines will become a hot topic in the light of the upcoming aviation emission regulations.

The main gaseous pollutants from aero-engines are carbon monoxide (CO), nitrogen oxide (NO_x) and unburnt hydrocarbon [12, 13]. Fu *et al*. and Kyprianidis *et al*. [14, 15] employed lean-burn combustors in aero-engines and obtained significant NO_x reduction. Zhang *et al.* [16] introduced a novel double-vortex combustor for gas turbine engines burning kerosene and lower emissions of CO, NO_x and UHC especially at high inlet temperature have been achieved. Numerical study was conducted by Hamed *et al.* [17] in order to figure out the

method to reduce NO_x emission of aero-engine combustor. Results indicated that the increase of the axial distance of the stabilizer and the number of holes could significantly hinder NO_x generation in the combustor [17]. Xing *et al*. [18] also summarised researches on reducing NO_x with increasing thermal efficiency via flameless combustion technologies. However, these methods of reducing gaseous emissions depend on retrofitting current aero-engines, which increase the costs of commercial application.

Another major pollution from aero-engines is the PM emissions including soot and volatile particles, which now contribute about 4.9% of total anthropogenic PM emissions, which have drawn increasing attentions in recent years [19, 20]. Ultrafine particles (smaller than 100 nm) are harmful to human health because they can penetrate deeply in the lung and alveoli [21, 22]. The size distributions and chemical compositions of PM emissions from gas turbines or aero-engines are the main research topics of scientists at present. The formation of ultrafine particles is highly correlative with fuel properties and engine operational conditions [13, 20, 23]. Lobo *et al*. [20] studied PM emissions of a JT8D-219 engine burning kerosene Jet A at various conditions. Results demonstrated that the mean diameter increased with increasing engine thrust and the PN emissions experienced a U shaped line when the engine power raised from about 4% to full level. Huang *et al.* [23] tested the aviation kerosene JP-8 and several renewable fuels in a jet engine. Higher PN concentrations were found at 85-100% power level than that of 4-7% power due to a higher fuel air ratio and the presence of aromatics content [23]. Timko *et al.* [24, 25] also demonstrated that PM emitted from aero-engines during take-off and landing played a dominant role in the ultrafine particle emissions (4−100 nm). And the majority of total PN concentrations was the nucleation mode

particles (5-50 nm) [24, 25]. However, in terms of engine operational parameters, previous researches have focused more on heavily sooting conditions (such as take-off, climb) and conditions that primarily affect the airport air quality (such as landing, taxiing). Limited researches have been conducted on the PN emissions under cruising and ground idling conditions, which represent the two longest durations of engine operation time.

The ion analysis can identify the water-soluble inorganic component such as metal ion, sulphate, nitrate and ammonium, which are the chemical source of toxicity in PM [26, 27]. Popovicheva *et al.* [28] tested kerosene with the sulphur content of 0.11 % in an aero-engine and reported that sulphates (SO_4^{2-}) and organic ions dominated the water-soluble fractions of soot emissions. Kinsey *et al.* and Mironova *et al*. [29, 30] demonstrated that $SO4^{2-}$ was the largest single component ion in particle emissions from aero-engines. Cl^{-}, NO^{3-}, NH_4^{+}, K^{+}, and Na^{+} as well as other metal elements were also found and their sources were considered the compositions of kerosene, engine lubrication oils and abrasion from engine wearing components [31, 32].

Biofuels are recognised as alternative energy resources for aero application, which could effectively mitigate the pollutant emissions from gas turbines or aero-engines. Chiaramonti *et al.* [33] tested diesel fuel, vegetable oil and biodiesel in a modified micro gas turbine and found that the combustion of vegetable oil generated comparable emissions with diesel fuel [33]. Habib *et al.* [34] tested four types of biofuels and their blends with Jet A in a gas turbine engine and demonstrated that biofuels decreased thrust-specific fuel consumption, CO and NO_x emissions. Mendez *et al.* [13] selected butanol as a typical biofuel and observed less NO_x and CO emissions. Seljak *et al.* [35] investigated the emissions of liquefied

lignocellulosic biofuels in a gas turbine and found out the NO_x and PMs are both reduced but the CO and UHC are increased. Nevertheless, a number of biofuels have shortcomings such as high viscosity, high surface tension and poor thermal stability, which may exert a negative impact on atomisation and combustion [36]. Jenkins *et al.* [37] and Chuck *et al*. [38] examined certain properties of several single-composition biofuels and compared with fossil fuel counterparts. Results suggested that butyl butyrate as a qualified biofuel surrogate, has similar viscosity, flash point, distillation profile and low temperature behaviour to kerosene (Jet A) [37, 38]. Thus the butyl butyrate has the potential to be used in a blend and fully compatible with aviation kerosene. However, experimental work on the combustion performance in gas turbine burning butyl butyrate-based biofuels has been rarely found in the literature.

In summary, gaseous and particulate matter (PM) emissions from gas turbine engines, which are highly correlative with the fuel compositions and operating conditions of engines, are drawing concerns due to the adverse effects on health and environment. However, most research work has not mentioned the information on PM number (PN) concentration at cruising state and idling state of aero-derivative gas turbine engines. In addition, biofuels have the advantage in reducing most pollutant emissions, yet most of them have poor viscosity, distillation profile and low temperature behaviour, which have negative impacts on atomization and combustion. Given the above considerations, a series of experiments on a gas turbine combustor were conducted to analyse the characteristics of CO, NO_x, unburnt hydrocarbon (UHC) and PM emissions of biofuels consisting of ethanol and butyl butyrate, which has closed thermal properties to aviation kerosene. Two conditions of the combustor

were operated to represent the cruising state and idling state of a gas turbine engine respectively.

2. Apparatus and Methodologies

2.1 Test rig and measurement instruments

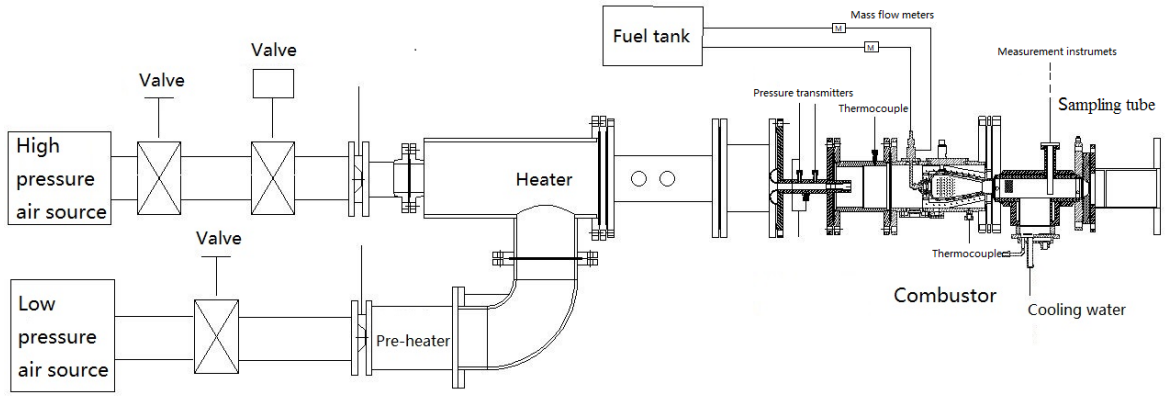

Fig. 1. Schematic of the test combustor rig

The gas turbine combustor consists of a high-pressure air source, a low-pressure air source, a combustion chamber, a fuel delivery system, and a cooling system. The schematic of the test combustor rig is show in Fig. 1. The pressure of air source is from 0 to 7 MPa and the air temperature can be heated up to 600 K. The fuel supply system with the injection pressure at 2 MPa consists of a main feed line and a secondary feed line respectively for the primary combustion and pre-combustion. The K-type thermocouples are employed to measure temperatures and pressure transmitters are used to measure the air pressures. The measured temperature and pressure conditions are used to calculate the air flow rate, which has the relative errors within 1.5%. Two Coriolis mass flow meters are used in the fuel supply lines to measure the fuel mass flow rate with the relative error of 1%.

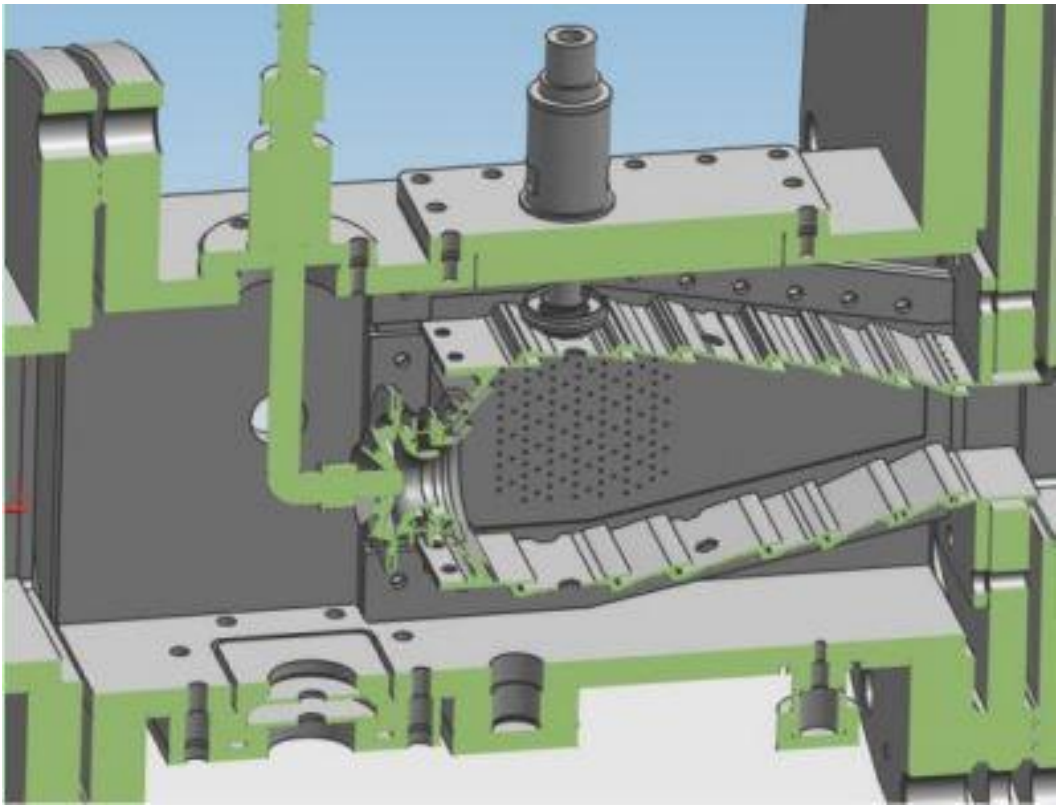

Fig. 2. The section view of the combustion chamber

The combustor in the combustion chamber is fabricated based on a typical aero-engine, whose section view is shown in Fig. 2. The case of the combustion chamber is 172 mm high and 325 mm long with the thickness and width of the case wall being 11 mm and 145 mm, respectively.

A sampling tube inserted inside the exhaust pipe of the combustion chamber was connected with an auto-controlled dilution system, which provides a precise control over the dilution condition (e.g. dilution ratio, dilution temperature, and residence time). There were two instruments downstream the dilution system, namely, a filter holder with a Whatman 47 mm GF/A filter for collecting the PM emissions, and a TSI 3936 Scanning Mobility Particle Sizer (SMPS) system for measuring the particle size resolved number concentrations. The reasons

for placing the dilution system prior to the filter and SMPS are:

1) Reduce the PM concentration and avoid particle collision, aggregation and deposition, which will cause a considerable change of PN

2) Stabilise the flow rate and reduce the humidity of exhaust gas in case of condensation

3) Ensure the PN concentration, the temperature and pressure of exhaust gas within the measurement range of the SMPS.

The SMPS system consists of a Differential Mobility Analyser (DMA) and a Condensation Particle Counter (CPC). Particles in the exhaust gas are classified into different particle size ranges by the DMA and then each class of particles are counted via the CPC to produce size distribution data. The measurable size range of the SMPS is 5 to 1000 nm. A gas analyser measures the gaseous emissions (CO, NO_x and UHC). The parameters of the gas analyser and its key components are listed in

Table **1**.

Table 1
The main components and parameters of the gas analyser

Gas analyser	Gas species	Range (ppm)	Accuracy
SIEMENS ULTRAMAC 6 OXYMAT 6	$CO/O_2/CO_2$	0 ~ 50000	±2%
CAI Model 600 CLD	NOx	300/1000	±1%
BASELINE 9000	UHC	200/2000	±1%

Filter borne PM samples were analysed by two ion chromatograph systems (DIONEX ICS2500 / DIONEX ICS2000, Dionex Company, USA) for water soluble ions or acids. Anions and organic acids were measured by a Dionex AS1 separator column and an ASRS ULRTA II 4 mm suppresser, with KOH solution as an eluent passing at 1.2 mL/min.

Information on cations were obtained by a Dionex CS-12 separator column and the CSRS ULRTA II 4 mm suppresser, with MSA (20 mmol/L) at 1.0 mL/min. The detailed parameters of the chromatograph system are listed in Table 2.

Table 2
Chromatograph systems for ions analysis

System mode	DIONEX ICS2500	DIONEX ICS2000
Destination	Cations	Inorganic anions & organic acids
Chromatograph column	IonPac CS12 separator column, 250mm×4mm	IonPac AS1 separator column, 250mm×4mm
Suppresser mode	CSRS ULTRA II 4mm	CSRS ULTRA II 4mm
Eluent	MSA solution, 1mL/min	KOH solution, 1.2mL/min
Volume	Auto inlet, 99μL	Auto inlet, 100μL

2.2 Methodologies

2.2.1 Fuel formulation

Because of the aforementioned reasons, butyl butyrate was chosen to be the primary component of test fuels. However, the poor volatility and higher surface tension of butyl butyrate may exert a negative impact on atomization and combustion. Because ethanol has a better volatility and was found to burn stably in gas turbines and produce less NO_x [39], the biofuel blends use the mixture of butyl butyrate and ethanol with different blending ratios. The ethanol fraction was chosen to be 0~50%. BB stands for butyl butyrate, and its ethanol blends are termed as BE-10, BE-30 and BE-50 with the number representing the volumetric fraction of ethanol. The aviation kerosene RP-3 was used as a reference. Relevant physical and chemical properties of the test fuels are listed in Table 3.

Table 3
Properties of the test fuels

Fuels	Mean formula	Viscosity (mm^2/s)	Surface tension (mN/m)	Density (g/cm^3)	Energy density (MJ/kg)

BB	$C_8H_{16}O_2$	1.194	26.41	0.8692	35.0
BE-10	$C_{6.56}H_{13.6}O_{1.76}$	1.166	24.81	0.8612	34.1
BE-30	$C_{5.43}H_{10.51}O_{1.45}$	1.157	23.84	0.8457	32.3
BE-50	$C_{3.56}H_{8.61}O_{1.26}$	1.130	22.77	0.8296	30.5
RP-3	$C_{10.35}H_{20.83}$	1.255	25.32	0.7967	42.8

2.2.2 Description of experimental procedure

The operating conditions 1 and 2 (Table 4) are based on the representative inlet parameters of the combustor at cruising state and idling state of an aero-engine.

Table 4
The operating conditions of the combustion chamber

Operating conditions	Inlet temperature (K)	Inlet pressure (MPa)	Inlet air flow (kg/s)	Fuel/air ratio (converted with kerosene)	Pressure drop
1	600	2	1.6	0.027	5.0%
2	520	0.5	0.5	0.015	5.0%

The experimental procedure can be described as the following steps:

1) Switch on the high pressure and low pressure air supply lines; turn on the fuel supply system and measurement instruments.
2) Ignite and adjust the combustor to the cruising state (condition 1);
3) When the gas flow in the dilution system became stable, the inlet of SMPS with the sampling flow 1.5 L/min is opened to measure the PM size distributions for one minute, and then the outlet of dilution system is switched to the filter holder to collect PM for five minutes;
4) The outlet of dilution system was switched off, and then the parameters of inlet air and fuel pressure was gradually adjusted to the idling state (condition 2);

5) Repeat step 3;
6) Stop feeding fuel, turned off the gas analyser and SMPS, and then keep the blowing air on until the combustion chamber cooled down;
7) Measure the weight of the filters before and after the tests, cut into pieces and put into beakers with deionized water, and then water-soluble inorganic ions and low molecular weight organic acids were analysed after a 30 min-ultrasonic extraction.

2.2.3 Data processing

The number-based emission index EI_n (#/kg) is used to estimate the level of PN emissions regardless of the quantity of consumed fuel, as shown in Equation (1)

$$EI_n = PN/m_f \quad (1)$$

Where PN refers to the total PN concentration (#/cm^3) and m_f is the mass of burnt fuel (kg). Meanwhile, the CO_2 production by the combustion of the fuel can be presented by following equation

$$m_{co_2} = \frac{PVM_{co_2}}{RT} \quad (2)$$

The m_{co_2}, V and M_{co_2} in the Equation (2) refer to the mass (g), volume (m^3) and molar mass (g/mol) of CO_2, respectively. R is the gas constant, and T and P are the absolute temperature (K) and pressure (Pa) in the combustor.

As m_{co_2} is determined by m_f and the carbon and hydrogen content in the fuel formula, these equations above can be combined and the number-based emission index EI_n could be confirmed in literature [20] as shown in Equation (3):

$$EI_n = PN \times 10^6 \frac{0.082T}{[CO_2](M_C + \alpha M_H)P} \quad (3)$$

Where M_C and M_H are the molar mass of carbon and hydrogen (g/mol); α is the hydrogen to carbon ratio of the fuel; $[CO_2]$ means the concentration of CO_2 emission (ppm) measured by the SIEMENS ULTRAMAC 6 OXYMAT 6. The total PN concentration can be obtained by numerically integrating the size-resolved number concentrations measured by the TSI 3936 SMPS system.

3. Results and discussion

3.1 Gaseous pollutant emissions

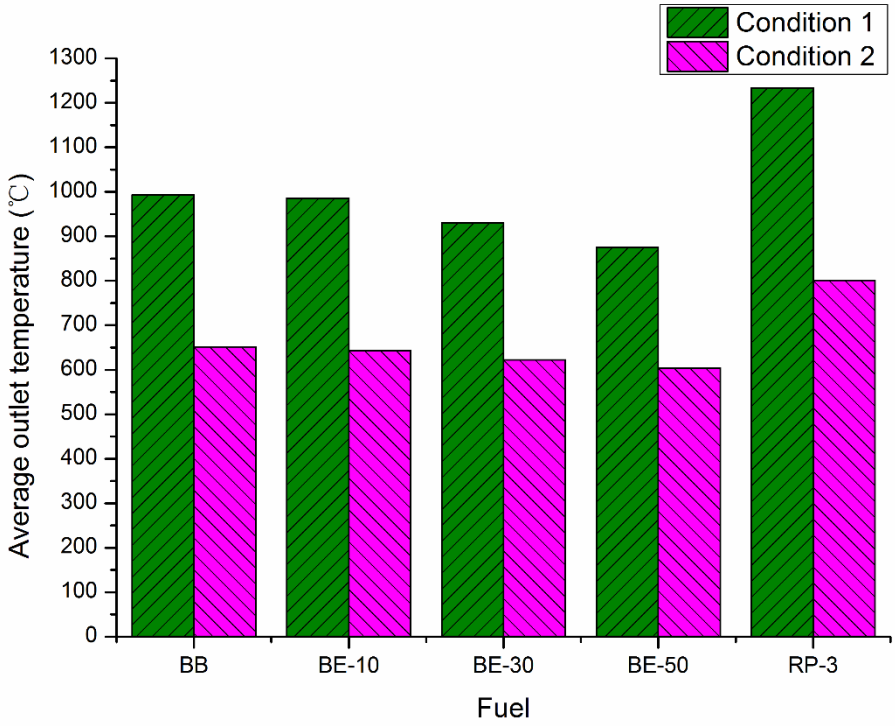

Fig. 3. Average outlet temperature of the combustion chamber

The emissions of CO, NO_x and UHC were measured at condition 1 (cruising state) and 2 (idling state). As the outlet temperature is an important factor indicating the combustion temperature, which influences both gaseous emissions and PM emissions, the average outlet temperature of the combustion chamber was measured and drawn in Fig. 3. The average outlet temperature of RP-3 were 1234℃ and 801℃ under condition1 and 2, respectively,

whilst biofuels exhibited noticeable lower (about 19.5%) average outlet temperature than RP-3. Because RP-3 has higher energy density than butyl butyrate and ethanol, more heat can be produced from burning RP-3 under the same fuel air ratio compared with that of other testing samples. Results indicated the increase of ethanol fraction in the biofuel blends, the average outlet temperature of the combustion chamber was reduced, which was caused by low heat value of ethanol.

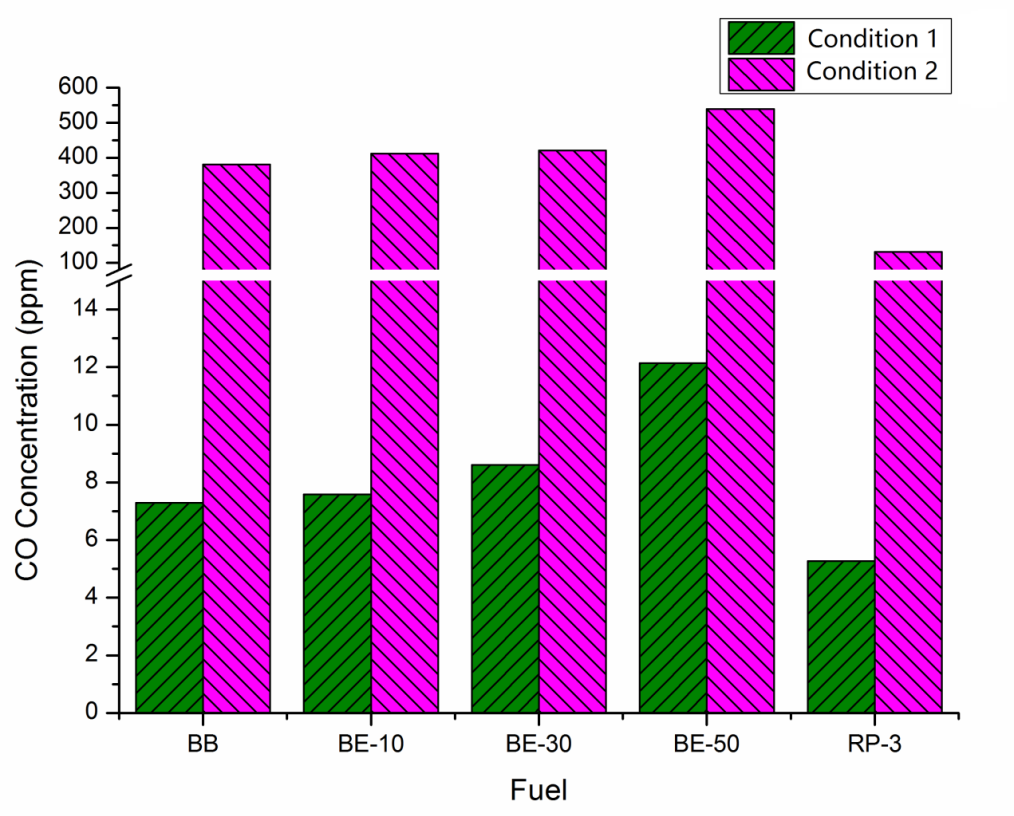

Fig. 4. The concentration of CO under two conditions

Fig. 4 shows the CO concentration from the four biofuel blends and reference fuel RP-3. The CO emissions from biofuel blends were all higher than that of RP-3 under the test conditions. Moreover, results indicated the CO emission under the engine idling state (condition 2) was

much higher than that under engine cruising state (condition 1).

CO is almost produced by pyrolysis at incomplete combustion, which can be concluded as[40]:

$$RH \rightarrow R \rightarrow RCHO \rightarrow RCO \rightarrow CO \quad (4)$$

Where R refers to radicals in fuel molecules. CO can be further oxidised to CO_2 via two different paths, which only dominate at high temperature with high reaction rate and efficiency and lower temperature with low reaction rate and efficiency, respectively. Given the measured outlet temperatures as shown in Fig. 3, the theory agrees well with the phenomenon in Fig. 4 that CO emission was much more at low power and biofuel blends with higher ethanol fractions led to higher CO emissions under the same power level.

As CO is mainly generated in low temperature zones, another possible reason for the tendency of CO emission is that ethanol has high volatility and high latent heat of vaporization. The vaporisation of ethanol during the injection induced longer ignition and increased overly lean regions, thus reduced the local combustion temperature and produced more CO.

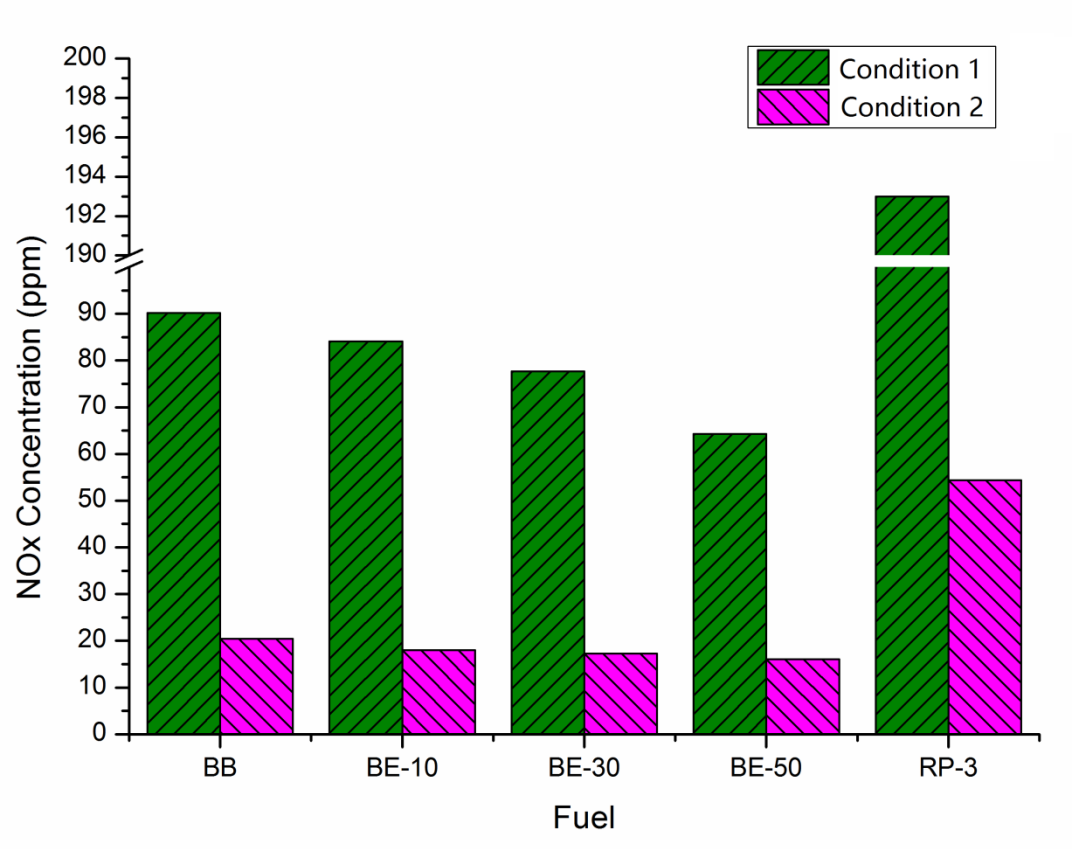

Fig. 5. The concentration of NO_x under two conditions

Compared with CO, the emission of NO_x experienced an opposite trend as shown in Fig. 5. NO_x at condition 1 was much higher than that at condition 2 for all fuels due to the significant influence of combustion temperature on NO_x formation. As summarised in literature [34, 40], three mechanisms determine the production of NO_x, the Thermal NO_x (T-NO), Prompt NO_x (P-NO) and Fuel NO_x (F-NO), among which the T-NO is dominant at high temperature and produces the most NO_x in combustion at high engine power according to Fig. 3. Similarly, the reduction of NO_x of biofuel blends [13], especially those with higher ethanol fraction, was also attributed to the lower combustion temperature caused by lower energy density of butyl butyrate and ethanol, which was caused by the presence of oxygen.

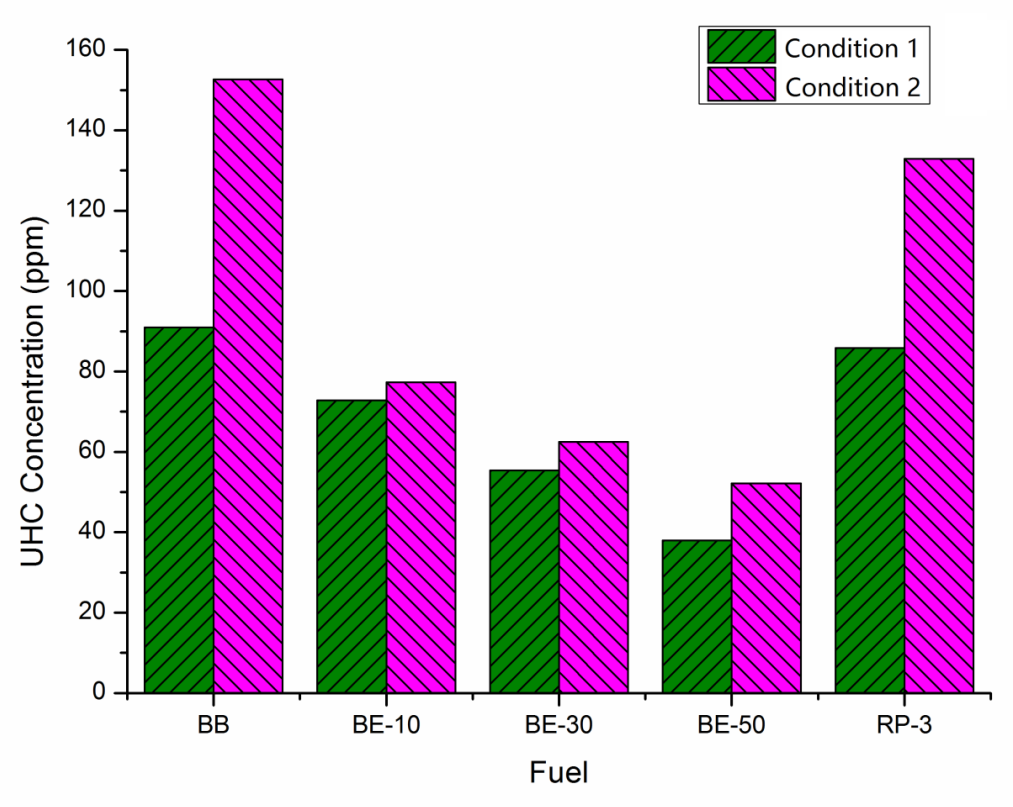

Fig. 6. The concentration of UHC under two conditions

Unburnt hydrocarbons (UHC) are the mixture of unburnt fuel vapour and the products of the thermal degradation of the parent fuel into lighter species, which are normally associated with poor atomisation, inadequate combustion, the effects of cooling air and the oxidation effect by the oxygen content in fuel compositions. For all the biofuel blends, a declining trend along the increasing engine load can be observed due to the higher combustion temperature under condition 1 as shown in Fig. 6. Although the higher latent heat of evaporation of ethanol in biofuels would reduce combustion temperature and thus promote UHC emissions, BE-10, 30, 50 produced lower UHC than RP-3 and BB under the test conditions. Lefebvre [40] suggested that the oxygen in fuels tends to oxidase the light fuel molecules at high temperature and thus significantly reduces UHC emission. It is conceivable that the oxidation of unburned hydrocarbon by the oxygen compositions in fuels was more significant than the

impact of combustion temperature as the difference of outlet temperature was not large among different biofuels. However, BB exhibited higher UHC emissions than RP-3 under condition 2 because the difference of combustion temperature was larger than that among biofuels but the effect of BB oxidation was not so strong due to its lowest oxygen content compared to other biofuels. In addition, UHC is likely to form particulate matter (PM) via a series of dehydrogenation and carbonization reactions, which can only happen at high temperature.

3.2 PM emissions

3.2.1 Size resolved number concentrations

The SMPS system was used for continuous measurement of number concentrations with the particle size range of 5~1000 nm. Since the number concentration of particles larger than 100 nm was nearly the same as that in the atmosphere and sub-15 nm data were subject to high noise-to-signal ratios, only 15~100 nm particles were selected and presented.

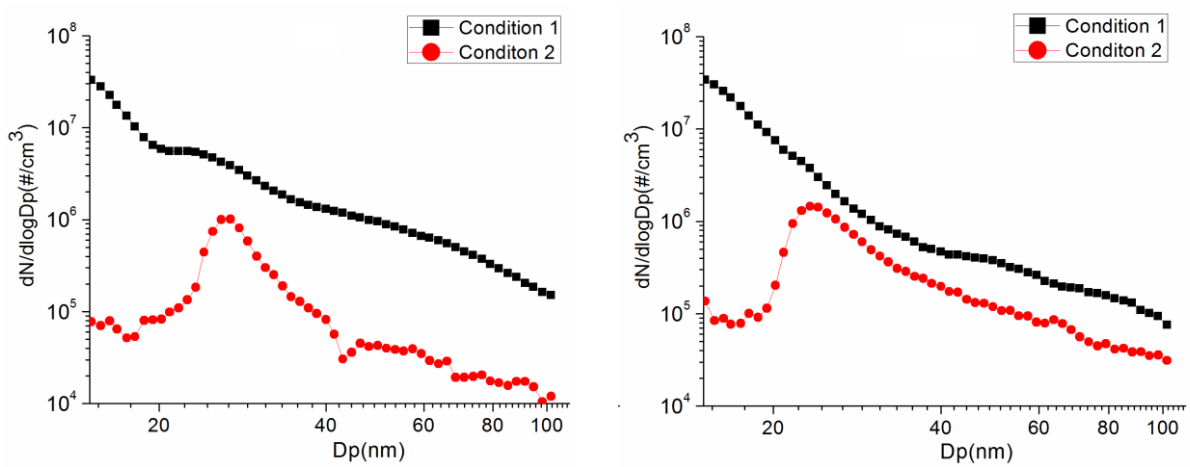

(a) (b)

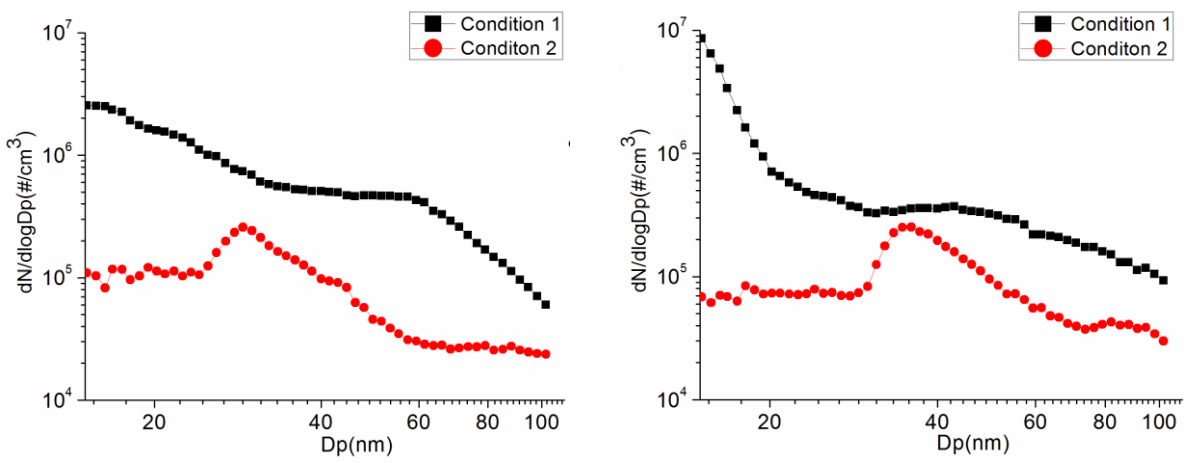

(c) (d)

Fig. 7. Size resolved number concentrations of PM emissions on a semi-logarithmic scale for four biofuels (a) BB ; (b) BE-10; (c) BE-30; (d) BE-50 under two conditions

(c) (d)

Fig. 7. Size resolved number concentrations of PM emissions on a semi-logarithmic scale for four biofuels (a) BB ; (b) BE-10; (c) BE-30; (d) BE-50 under two conditions

illustrates the PM emissions of the four test fuels under the two operating conditions. Results indicated sub-20 nm particles (in nucleation mode) dominated the size spectrum for the biofuels at condition 1. The size resolved number concentration experienced continuous decline when particles were larger than 20 nm. In contrast, particles under condition 2 had much fewer number concentrations than that under condition 1 and reached peak in the range of 30 ~ 40 nm.

The peak of the size spectra occurred for each fuel under condition 2 and moved from ~25 nm to ~40 nm when ethanol proportion increased from 10% to 50%. The reason might be that as ethanol addition increased, the elevated oxygen content of the blends would have promoted the oxidation of nucleation mode PM (particles smaller than 50 nm) whilst affected

the accumulation mode PM (50-500 nm) to a less extent. However, BB did not follow the trend with its peak size larger than that of BE-10. It could be attributable to the fact that BB produced more UHC than BE-10 (Fig. 6), which means less UHC emitted from BB combustion formed small particles via dehydrogenation and carbonization so that the peak of the BB size spectra moved towards a larger size compared with BE-10.

The particle number concentrations of the four biofuels over the entire size range under condition 1 were all higher than those under condition 2. This indicates that cruising state played a relatively dominate role in PM emissions than idling state, because the relatively fuel-rich combustion at cruising state (high fuel air ratio) increases the likelihood of incomplete combustion in some zones of the combustor and particle formation via polymerisation and dehydrogenation. The much lower PM emissions under idling were caused by leaner combustion, which means more oxygen was available to promote the PM oxidation and mitigate the dehydrogenation of organic molecules.

By integrating the above PN spectra, the total PN concentration can be obtained. With CO_2 emissions data, the emission index of total particulate number concentration (EI_n) under two operating conditions can be calculated via Equation (3) and the results are shown in **Error! Reference source not found.**.

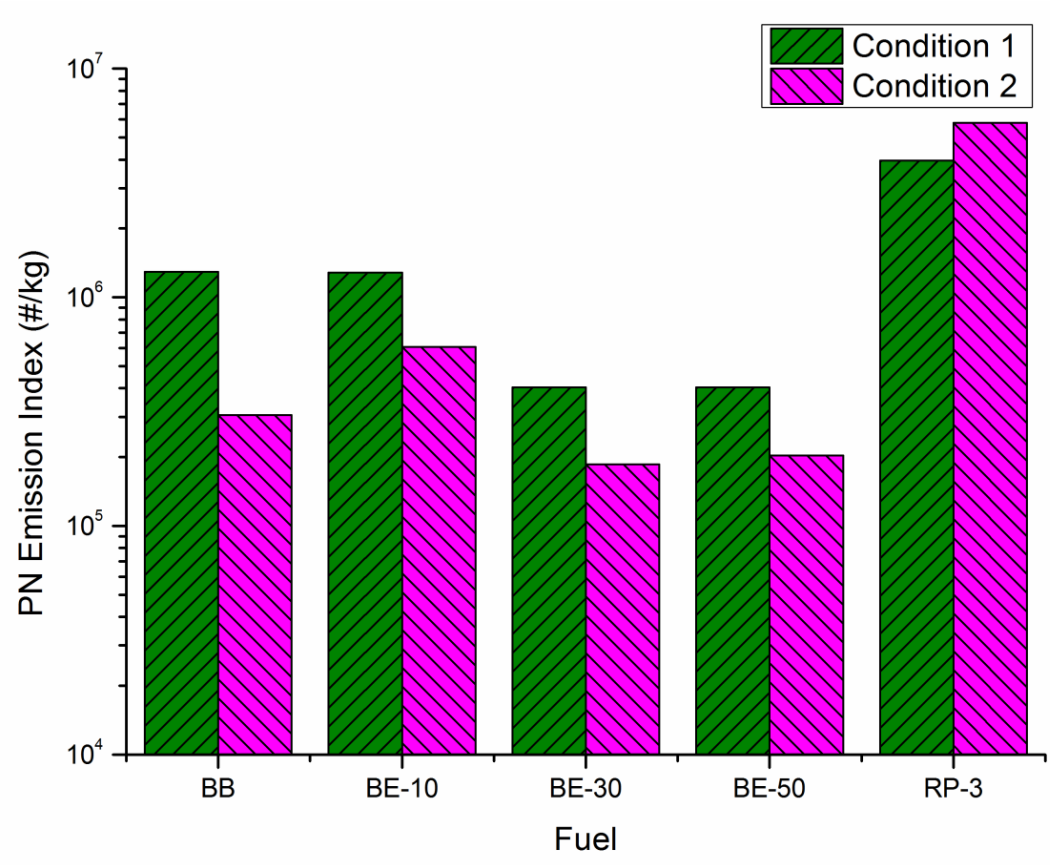

Fig. 8. The emission index of total particulate number concentrations for different test fuels under two conditions

Both

(c) (d)

Fig. 7. Size resolved number concentrations of PM emissions on a semi-logarithmic scale for four biofuels (a) BB ; (b) BE-10; (c) BE-30; (d) BE-50 under two conditions

and Fig. 8**Error! Reference source not found.** illustrated that the emission level of PN concentration under condition 1 are all higher than that of condition 2, when the four biofuels are used in the combustor. However, the RP-3 shows an opposite tendency.

Previous research [20] on PM emissions of fossil fuels in aero-engines demonstrated that a U-shaped line regulation of PM emissions versus engine power level, which means the PM emissions are usually higher at idling state (4% ~ 7% power level) and reduce to its minimum at about 15% ~ 30% power level, and then increase again. In this research, PM emissions

between four biofuels and RP-3 are slightly different but both in accordance to the U-shaped line. Moreover, literature [41-44] also suggested that different fuels have different U-shaped lines, where fossil fuels usually have two equal ends for both lowest and highest power level but alternative fuels tend to have a higher end at high power level. The reasons can be summarised as

1) Alternative fuels, especially biofuels, are more difficult to ignite due to lower energy density and thus aggravate the incomplete of combustion in the fuel rich zones at high fuel air ratio and air flow at cruising state. RP-3 has higher combustion temperature, whose effect could surpass that of rich fuel and boost combustion process at cruising state

2) Polycyclic aromatic hydrocarbons (PAH) and sulphur in RP-3 are the two main factors for PM formation at lower temperature in idling state, compared with the dehydrogenation and carbonisation reactions of UHC at higher temperature, but biofuels have no PAH and sulphur.

As indicated in Fig. 8**Error! Reference source not found.**, RP-3 produced more particles at idling state because it contains a high proportion of PAHs, whilst the opposite tendency of PM emissions of the four biofuels can be attributed to the lack of PAHs and sulphur. The dehydrogenation and carbonization reactions of UHC under cruising state (higher temperature) is likely to be a more significant factor influencing PM formation for biofuels.

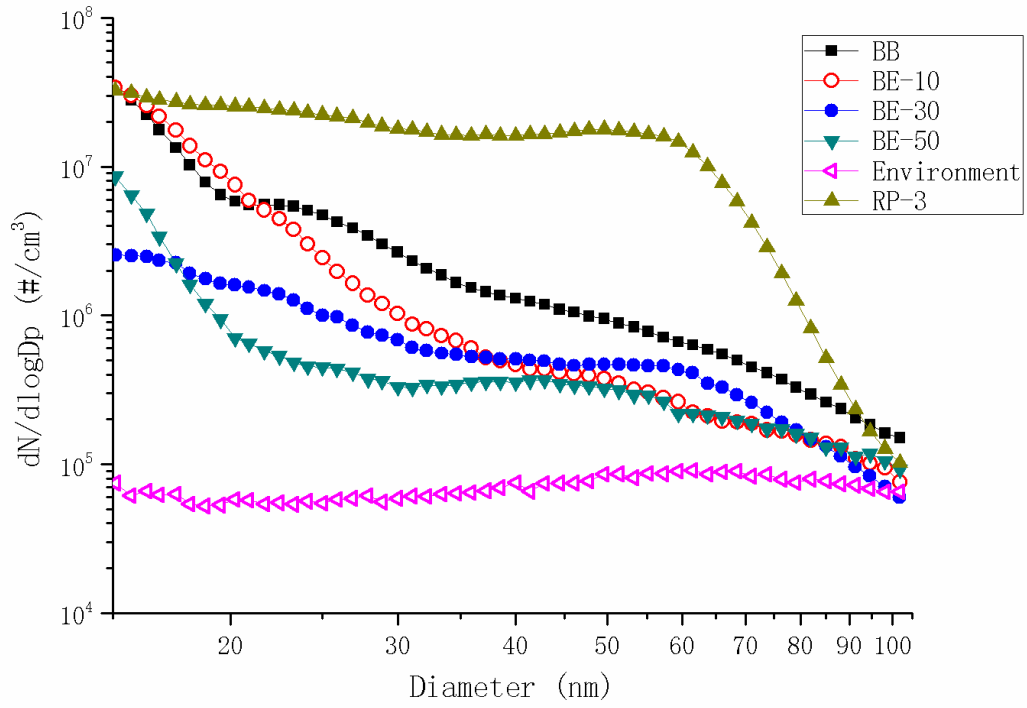

Fig. 9. Comparison of different test fuels in relation to PM size distributions under condition 1

Results shown in **Error! Reference source not found.** and Fig. 9 also indicate that increased ethanol content tends to reduce PM emissions. The relatively high oxygen content in ethanol molecules can accelerate soot oxidation to carbon dioxide in combustion. On the other hand, ethanol addition improves the quality of spray atomization, because its lower viscosity and surface tension as well as higher volatility enable the liquid fuel to break up into finer droplets and evaporate in a shorter time, which results in a more uniform fuel-air blend and more complete combustion. Since the energy density of ethanol is less than that of butyl butyrate, fuels with higher ethanol proportions cannot generate flames of such high temperature. This feature can also reduce particles because organic molecules cannot be dehydrogenated at lower temperature, as conjectured in Fig. 6. The combination of aforementioned factors causes the inhibition of PM production when ethanol is blended.

3.2.2 Ions analysis

As the amount of particles collected by Teflon films under operational condition 2 was much less than that under operating condition 1, only the latter was analysed. Each filter was cut into two pieces for two groups of ions analysis. Five inorganic cations (NH_4^+, Ca^{2+}, Na^+, Mg^{2+}, K^+), three inorganic anions (Cl^-, NO_3^-, SO_4^{2-}) and five low molecular weight organic acids (formic acid, acetic acid, propionic acid, oxalic acid, succinic acid) were quantitatively determined from filter borne PM samples.

The mass concentration of five cation ions was obtained by analysing half filters in CS-12 separation column, whilst three inorganic anions and five organic acids were analysed by using the AS1 separation column. The calculated molar fractions of all ions and organic acids are shown in Fig. 10.

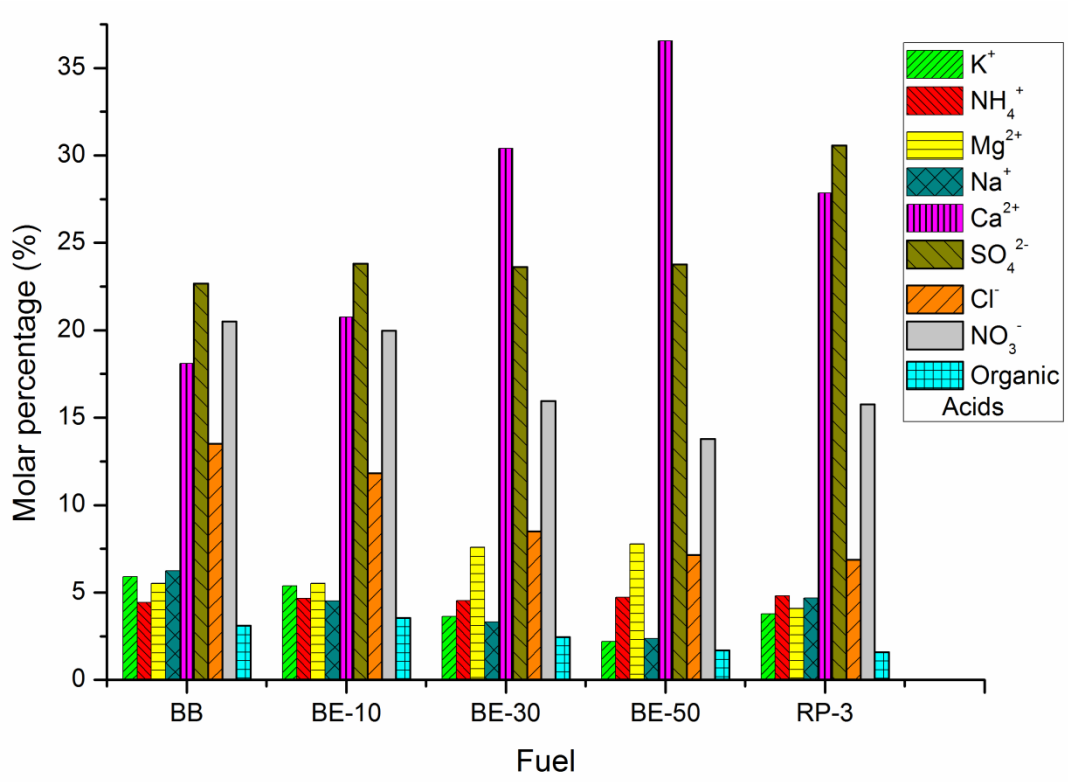

Fig. 10 Molar fractions of individual ions and organic acids analysed from filter borne PM samples of different test fuels under condition 1

Fig. 10 shows that Ca^{2+} was the majority ion among the five cation ions and its molar percentage increased monotonically from 18.11% to 36.55% with the increase of ethanol content. In contrast, the percentage of K^+ and Na^+ exhibited a gradually decreasing trend from 5.90% to 2.21% and 6.24% to 2.35% as the fraction of butyl butyrate dropped, because K^+ was believed to come from biomass combustion. The three cation ions accounted for 27.85%, 3.78% and 4.68% respectively for RP-3 PM emissions. The molar percentages of Mg^{2+} and NH_4^+ were rather stable for all test fuels with the range of 4.09% ~ 7.77% and 4.43% ~ 4.81, respectively.

As to the inorganic anions, SO_4^{2-} was the dominant anion with the fraction of approximately 23% for all the BE fuels, whilst the kerosene RP-3 produced a higher percentage of 30.57%. This may be caused by the oxidation of sulphur, which is a common impurity in kerosene (RP-3) and lubrication oil. NO_3^- was the second highest anion and it declined from 20.50% to 13.79% with the increase in ethanol content. This may be because that the existence of ethanol reduced the combustion temperature due to its low energy density, which inhibited the oxidation of nitrogen to NO_x, the precursor of NO_3^-. Similarly, the percentage of Cl^- experienced a gradually decreasing trend and some Cl species in lubrication oils were probably the main sources of Cl^-.

The total percentage of the five organic acids was no more than 3.55% for all the test fuels with the minimum of 1.6% found in RP-3 PM emissions. Previous studies suggested that low molecular weight organic acids are mainly attributed to photochemistry conversion in the wet atmosphere [45]. However, the production of organic acids in this study was believed to originate from the hydrolytic reactions of unburnt butyl butyrate at high temperature, which

was prohibited by the increase of ethanol fraction. The fact that the overall amount of organic acids was much smaller than that of inorganic ions implied complete combustion of the test fuels.

4. Conclusions

This paper reports the gaseous and particulate matter (PM) emissions and icon analysis of burning a promising bio-jet fuel (butyl butyrate) for aviation engine using a gas turbine combustor. Two engine operational conditions (cruising and idling state) were conducted to study the potential of using butyl butyrate-based biofuels as alternative clean bio-jet fuels for aero-engines application. The results drawn from this work can be summarised as,

1. The concentration of CO emissions from biofuel blends was significantly higher than that of RP-3 during both cruising and idling states. The increase of the ethanol content in the biofuels led to a rise of CO emissions.
2. The biofuel blends effectively reduced the NO_x emissions by up to 70.4% compared with RP-3 under both cruising and idling states. The increase of ethanol fraction could further depress the NO_x emissions.
3. Biofuels produced less UHC than RP-3 by at most 60.9% (BE-50) except for pure butyl butyrate. The combustion temperature and the oxidation effect by oxygen compositions in the fuels are two primary factors influencing UHC emissions.
4. To all biofuels, particles smaller than 20 nm dominated PN emissions under cruising state, and the concentrations decreased dramatically as particle size increased larger than 20 nm. In contrast, the size resolved number concentrations under idling state were much less and each fuel exhibited a peak value between about $2\times10^6/cm^3$ and $3\times10^6/cm^3$ in

the range of about 25 nm to 40 nm. The emission index of total PN concentrations for biofuels was significantly lower than that of RP-3.

5. Ca^{2+} turned out to be the majority ion among the five cation ions and its molar percentage increased from 18.1% to 36.6% with increasing ethanol content. SO_4^{2-} was the main anion with a relatively stable content of approximately 23% for all the BE fuels.

Acknowledgement

This research is supported by National Natural Science Foundation of China (91641119 and 51306011). The financial supports from the SAgE doctoral Training Award NH/140671210 and from Chinese Scholarship Council under No. 201508060054 are also acknowledged.

Reference

[1] Amara AB, Dauphin R, Babiker H, Viollet Y, Chang J, Jeuland N, et al. Revisiting diesel fuel formulation from Petroleum light and middle refinery streams based on optimized engine behavior. Fuel. 2016;174:63-75.

[2] Chen L, Stone R, Richardson D. A study of mixture preparation and PM emissions using a direct injection engine fuelled with stoichiometric gasoline/ethanol blends. Fuel. 2012;96:120-30.

[3] Chen L, Zhang Z, Gong W, Liang Z. Quantifying the effects of fuel compositions on GDI-derived particle emissions using the optimal mixture design of experiments. Fuel. 2015;154:252-60.

[4] Chen L, Stone R, Richardson D. Effect of the valve timing and the coolant temperature on particulate emissions from a gasoline direct-injection engine fuelled with gasoline and with a gasoline–ethanol blend. Proceedings of the Institution of Mechanical Engineers, Part D: Journal of Automobile Engineering. 2012;226:1419-30.

[5] Tan P-q, Ruan S-s, Hu Z-y, Lou D-m, Li H. Particle number emissions from a light-duty diesel engine with biodiesel fuels under transient-state operating conditions. Applied Energy. 2014;113:22-31.

[6] Chen L, Liang Z, Zhang X, Shuai S. Characterizing particulate matter emissions from GDI and PFI vehicles under transient and cold start conditions. Fuel. 2017;189:131-40.

[7] Lee S, Kwak J, Lee S, Lee J. On-road chasing and laboratory measurements of exhaust particle emissions of diesel vehicles equipped with aftertreatment technologies (DPF, urea-SCR). International Journal of Automotive Technology. 2015;16:551-9.

[8] Mamakos A, Martini G, Manfredi U. Assessment of the legislated particle number measurement procedure for a Euro 5 and a Euro 6 compliant diesel passenger cars under regulated and unregulated conditions. Journal of Aerosol Science. 2013;55:31-47.

[9] Giechaskiel B, Wang X, Gilliland D, Drossinos Y. The effect of particle chemical composition on the activation probability in n-butanol condensation particle counters. Journal of Aerosol Science. 2011;42:20-37.

[10] Otsuki Y, Takeda K, Haruta K, Mori N. A Solid Particle Number Measurement System Including Nanoparticles Smaller than 23 Nanometers. SAE Technical Paper; 2014.

[11] Secretariat I. Annex 16—environmental protection volume II—aircraft engine emissions. ISBN 978-92-9231-123-0; 2008.

[12] D'Alessandro F, Pacchiarotta G, Rubino A, Sperandio M, Villa P, Carrera AM, et al. Lean Catalytic Combustion for Ultra-low Emissions at High Temperature in Gas-Turbine Burners. Energy & Fuels. 2011;25:136-43.
[13] Mendez C, Parthasarathy R, Gollahalli S. Performance and emission characteristics of butanol/Jet A blends in a gas turbine engine. Applied Energy. 2014;118:135-40.
[14] Fu Z, Lin Y, Li L, Zhang C. Experimental and numerical studies of a lean-burn internally-staged combustor. Chinese Journal of Aeronautics. 2014;27:488-96.
[15] Kyprianidis KG, Dahlquist E. On the trade-off between aviation NOx and energy efficiency. Applied Energy. 2017;185:1506-16.
[16] Zhang RC, Fan WJ, Shi Q, Tan WL. Combustion and emissions characteristics of dual-channel double-vortex combustion for gas turbine engines. Applied Energy. 2014;130:314-25.
[17] Zeinivand H, Bazdidi-Tehrani F. Influence of stabilizer jets on combustion characteristics and NOx emission in a jet-stabilized combustor. Applied energy. 2012;92:348-60.
[18] Xing F, Kumar A, Huang Y, Chan S, Ruan C, Gu S, et al. Flameless combustion with liquid fuel: A review focusing on fundamentals and gas turbine application. Applied Energy. 2017;193:28-51.
[19] Lee DS, Fahey DW, Forster PM, Newton PJ, Wit RC, Lim LL, et al. Aviation and global climate change in the 21st century. Atmospheric Environment. 2009;43:3520-37.
[20] Lobo P, Hagen DE, Whitefield PD, Raper D. PM emissions measurements of in-service commercial aircraft engines during the Delta-Atlanta Hartsfield Study. Atmospheric Environment. 2015;104:237-45.
[21] Moniruzzaman CG, Yu F. A 0D aircraft engine emission model with detailed chemistry and soot microphysics. Combustion and Flame. 2012;159:1670-86.
[22] Argyropoulos G, Samara C, Voutsa D, Kouras A, Manoli E, Voliotis A, et al. Concentration levels and source apportionment of ultrafine particles in road microenvironments. Atmospheric Environment. 2016;129:68-78.
[23] Huang C-H, Vander Wal RL. Effect of Soot Structure Evolution from Commercial Jet Engine Burning Petroleum Based JP-8 and Synthetic HRJ and FT Fuels. Energy & Fuels. 2013;27:4946-58.
[24] Timko MT, Onasch TB, Northway MJ, Jayne JT, Canagaratna MR, Herndon SC, et al. Gas turbine engine emissions—Part II: Chemical properties of particulate matter. Journal of Engineering for Gas Turbines and Power. 2010;132:061505.
[25] Mazaheri M, Johnson GR, Morawska L. Particle and gaseous emissions from commercial aircraft at each stage of the landing and takeoff cycle. Environmental science & technology. 2008;43:441-6.
[26] Mazaheri M, Bostrom TE, Johnson GR, Morawska L. Composition and morphology of particle emissions from in-use aircraft during takeoff and landing. Environmental science & technology. 2013;47:5235-42.
[27] Meng Q, Richmond-Bryant J, Lu S-E, Buckley B, Welsh WJ, Whitsel EA, et al. Cardiovascular outcomes and the physical and chemical properties of metal ions found in particulate matter air pollution: a QICAR study. Environmental health perspectives. 2013;121:558.
[28] Popovicheva O, Persiantseva NM, Shonija NK, DeMott P, Koehler K, Petters M, et al. Water interaction with hydrophobic and hydrophilic soot particles. Physical Chemistry Chemical Physics. 2008;10:2332-44.
[29] Kinsey J, Hays M, Dong Y, Williams D, Logan R. Chemical characterization of the fine particle emissions from commercial aircraft engines during the aircraft particle emissions experiment (APEX) 1 to 3. Environmental science & technology. 2011;45:3415-21.
[30] Mironova IA, Aplin KL, Arnold F, Bazilevskaya GA, Harrison RG, Krivolutsky AA, et al. Energetic particle influence on the Earth's atmosphere. Space Science Reviews. 2015;194:1-96.
[31] Demirdjian B, Ferry D, Suzanne J, Popovicheva O, Persiantseva N, Shonija N. Heterogeneities in the microstructure and composition of aircraft engine combustor soot: impact on the water uptake. Journal of

atmospheric chemistry. 2007;56:83-103.
[32] Abegglen M, Brem B, Ellenrieder M, Durdina L, Rindlisbacher T, Wang J, et al. Chemical characterization of freshly emitted particulate matter from aircraft exhaust using single particle mass spectrometry. Atmospheric Environment. 2016;134:181-97.
[33] Chiaramonti D, Rizzo AM, Spadi A, Prussi M, Riccio G, Martelli F. Exhaust emissions from liquid fuel micro gas turbine fed with diesel oil, biodiesel and vegetable oil. Applied energy. 2013;101:349-56.
[34] Habib Z, Parthasarathy R, Gollahalli S. Performance and emission characteristics of biofuel in a small-scale gas turbine engine. Applied Energy. 2010;87:1701-9.
[35] Seljak T, Oprešnik SR, Kunaver M, Katrašnik T. Wood, liquefied in polyhydroxy alcohols as a fuel for gas turbines. Applied energy. 2012;99:40-9.
[36] Sallevelt J, Gudde J, Pozarlik A, Brem G. The impact of spray quality on the combustion of a viscous biofuel in a micro gas turbine. Applied energy. 2014;132:575-85.
[37] Jenkins RW, Munro M, Nash S, Chuck CJ. Potential renewable oxygenated biofuels for the aviation and road transport sectors. Fuel. 2013;103:593-9.
[38] Chuck CJ, Donnelly J. The compatibility of potential bioderived fuels with Jet A-1 aviation kerosene. Applied Energy. 2014;118:83-91.
[39] Lefebvre AH, Ballal DR. Gas Turbine Combustion: Alternative Fuels and Emissions, 2010. CRC Press, Taylor & Francis Group). ISBN-13.
[40] Lefebvre AH. Gas turbine combustion: CRC press; 1998.
[41] Anderson B, Beyersdorf A, Hudgins C, Plant J, Thornhill K, Winstead E, et al. Alternative aviation fuel experiment (AAFEX). 2011.
[42] Bulzan D, Anderson B, Wey C, Howard R, Winstead E, Beyersdorf A, et al. Gaseous and particulate emissions results of the NASA alternative aviation fuel experiment (AAFEX). ASME Turbo Expo 2010: Power for Land, Sea, and Air: American Society of Mechanical Engineers; 2010. p. 1195-207.
[43] Moore RH, Shook M, Beyersdorf A, Corr C, Herndon S, Knighton WB, et al. Influence of jet fuel composition on aircraft engine emissions: A synthesis of aerosol emissions data from the NASA APEX, AAFEX, and ACCESS missions. Energy & Fuels. 2015;29:2591-600.
[44] Beyersdorf A, Anderson B. An overview of the NASA alternative aviation fuel experiment (AAFEX). TAC–2 Proceedings, 2nd International Conference on Transport, Atmosphere and Climate2009. p. 21-5.
[45] Hu M, Zhang J, Wu Z. Chemical compositions of precipitation and scavenging of particles in Beijing. Science in China Series B: Chemistry. 2005;48:265-72.